American Mineralogist, Volume 78, pages 1304–1312, 1993

Lindqvistite, $Pb_2MeFe_{16}O_{27}$, a novel hexagonal ferrite mineral from Jakobsberg, Filipstad, Sweden

Dan Holtstam*

Institute of Earth Sciences, Uppsala University, Norbyvägen 18 B, S-752 36 Uppsala, Sweden

Rolf Norrestam

Department of Structural Chemistry, Arrhenius Laboratory, Stockholm University, S-106 91 Stockholm, Sweden

Abstract

Lindqvistite is a new mineral from Jakobsberg, Filipstad, Sweden. It occurs as black crystals up to 5 mm in size with perfect basal cleavage, associated with hematite, jacobsite, plumboferrite, calcite, phlogopite, andradite, hedyphane, barite, and copper minerals. The mineral is opaque, gray in reflected light, with weak bireflectance, and it is moderately anisotropic. Reflectance values obtained in air and oil (at 589 nm) are R_o = 22.2, $R_{e'}$ = 21.5, $^{im}R_o$ = 8.76, and $^{im}R_{e'}$ = 8.34%. VHN_{100} = 857 and D_{calc} = 5.76(1) g/cm^3. The idealized formula for lindqvistite is $Pb_2MeFe_{16}O_{27}$, with Me = Mn^{2+}, Mg. An empirical formula based on microprobe analyses is $Pb_{2.04}Mn_{1.27}Mg_{0.71}Zn_{0.04}Fe_{14.84}Al_{0.02}Ti_{0.03}Si_{0.05}O_{26.51}$.

X-ray studies show that lindqvistite is hexagonal, essentially $P6_3/mmc$, with a = 5.951(1), c = 33.358(4) Å, and V = 1023.1(5) Å^3 for Z = 2. The eight most intense reflections in the X-ray powder pattern [d in ångströms (I/I_o)(hkl)] are 4.168(55)(008), 3.334(40)(0,0,10), 3.011(60)(109), 2.975(70)(110), 2.802(95)(1,0,10), 2.779(45)(0,0,12), 2.624(100)(116), and 2.612(90)(1,0,11).

Very weak diffuse extra reflections, about two orders of magnitude weaker than the substructure reflections, observed on X-ray photographs could be indexed with a tripled hexagonal unit cell ($a' = a \cdot \sqrt{3}$ = 10.31 Å and $c' = c$). The present investigation is confined to elucidating the substructure having a = 5.951 Å. The derived structural model of lindqvistite has been refined, with the 505 most significant X-ray reflections [$I > 5\sigma$ (I)] with (sin θ)/$\lambda \leq$ 0.81/Å to R = 0.041. It is closely related to the W-type synthetic ferrites and can be described in terms of two basic structural units, commonly denoted as the R and the S (spinel) blocks. The stacking sequence of such blocks is $RSSR'S'S'$, where R = $(Pb_2Fe_5O_{11})^{3-}$ and S = $(Me_{0.5}Fe_{5.5}O_8)^{1.5+}$ for lindqvistite. The two crystallographically different Pb atoms and a single O atom, all located at the central section of the R block, are positionally disordered.

The mineral name honors Bengt Lindqvist of the Swedish Museum of Natural History, where the type material is deposited.

Introduction

The hexagonal ferrites make up a large family of compounds with the general formula $mAO \cdot nMeO \cdot oFe_2O_3$, where A = Sr, Ba, or Pb and Me = Mg^{2+}, Mn^{2+}, Fe^{2+}, Co^{2+}, Zn^{2+}, etc. The most common space group symmetries encountered are $P6_3/mmc$ and $R\bar{3}m$. The phases have gained considerable scientific and technological interest, mainly as permanent magnets with high anisotropy. The crystal structure systematics of the family were investigated first by Braun (1952, 1957). Recent reviews on the subject include Kojima (1982) and Collongues et al. (1990). The hexagonal ferrites are primarily represented in nature by magnetoplumbite, $PbFe_{12}O_{19}$, and other members of the mineral group bearing its name. Structurally they are known as the M-type ferrites. The present paper reports on a new Pb-bearing hexagonal ferrite mineral from the Jakobsberg Fe-Mn deposit; it is related to the W-type synthetic ferrites ($AMe_2Fe_{16}O_{27}$), and it is identical with the phase noted by Kohn and Eckart (1969), for which they gave cell geometry and basic structure data.

The mineral, named lindqvistite in honor of Bengt Lindqvist (b. 1927), Senior Curator at the Swedish Museum of Natural History (NRM), was approved by the IMA Commission on New Minerals and Mineral Names prior to publication. Holotype material is preserved at NRM, Stockholm (catalogue no. 38126). A part of the holotype (polished mount) is deposited at the Natural History Museum, London (catalogue no. BM 1992,375).

* Address for correspondence: Department of Mineralogy, Swedish Museum of Natural History, Box 50007, S-104 05 Stockholm, Sweden.

0003–004X/93/1112–1304$02.00

Occurrence

The Jakobsberg mines (the older spelling is Jacobsberg) are located near Nordmark in the Filipstad district, central Sweden (59.83°N, 14.11°E). Mining activities took place sporadically during the 19th century, aimed primarily at extracting Mn ores, and finally ceased by the end of World War I (Tegengren, 1924).

Characteristic minerals for the deposit are hausmannite, jacobsite, hematite, phlogopite, diopside, aegirine augite, andradite, piemontite, celsian, various lead silicates, plumboferrite, native copper, and secondary Cu minerals. Typically the rocks have a banded appearance, with oxides and calcium and magnesium silicates concentrated in irregular layers, intercalated with parts rich in carbonates.

The ore bodies and associated skarn assemblages are hosted by dolomitic marble. It belongs to the stratigraphically lower parts (≥1.9 b.y. old) of a widespread Paleoproterozoic supracrustal rock sequence of volcano-sedimentary affinity. The Filipstad area underwent deformation and regional metamorphism during the Svecofennian orogeny, locally reaching amphibolite facies at the peak around 1.85 b.y. ago. Different generations of granitoids have intruded the supracrustal formation over the time span 1.85–1.77 Ga, providing thermal energy for further metamorphism (Björk, 1986).

The manifest geochemical and mineralogical similarities between Jakobsberg and the more famous Långban deposits (Moore, 1970) situated 9 km to the northeast, indicate that they are genetically related. According to contemporary knowledge, the iron manganese oxide mineralizations in the Filipstad district represent metamorphic equivalents of oceanic exhalative-sedimentary deposits (Boström et al., 1979; Damman, 1988).

Lindqvistite was found in a museum specimen (here designated the holotype), and subsequently a few samples have been recovered in mine dumps at Jakobsberg. It is associated with hematite, jacobsite, plumboferrite, phlogopite, andradite, calcite, hedyphane, barite, native copper, cuprite, malachite, and azurite. All minerals have been identified utilizing optical and X-ray methods.

Physical properties

Lindqvistite is opaque and black, with a submetallic luster. The mineral is brittle and leaves a brownish black streak on being powdered. It occurs as subhedral tabular crystals (0.2–5 mm in greatest dimension), flattened on {0001}, and exhibiting perfect cleavage along the same plane (Fig. 1). The holotype specimen is fairly rich in the mineral, and the crystals occasionally tend to form larger aggregates, where they occur intergrown with jacobsite and plumboferrite. There is a strong megascopic resemblance between lindqvistite and plumboferrite. The microindentation hardness, measured as VHN_{100}, is 857 (average of ten indentations, range 818–898), corresponding to a calculated Mohs hardness of about 6. It takes a polish less well than hematite and jacobsite. The calculated density is 5.76(1) g/cm³ for an empirical formula based on microprobe analyses (cf. the following). Lindqvistite is normally nonmagnetic. However, after heat treatment (840 °C for 3 h in air) it becomes moderately magnetic. It is slowly soluble in cold HCl 3:1 solution but is not affected by HNO_3 or H_2SO_4.

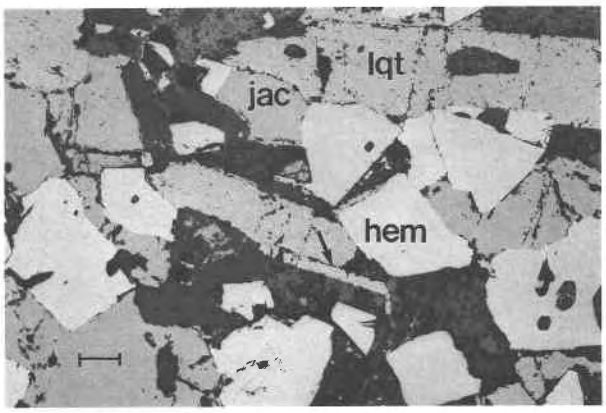

Fig. 1. Photomicrograph of sample no. 38126 (reflected light), with hematite (hem), jacobsite (jac), lindqvistite (lqt), and plumboferrite. The arrow points to a plumboferrite grain adjacent to lindqvistite. The low-reflecting phases are mainly mica, calcite, and hedyphane. Scale bar represents 0.1 mm.

Optical properties

In reflected, linearly polarized light (~3200 K) the mineral is gray with a faint brownish tint (compared with associated jacobsite, which has a distinct brownish tint). The bireflectance is weak, and no reflection dichroism is discernible. Internal reflections or twinning have not been observed. Lindqvistite shows a moderate anisotropy with polarization colors varying from bluish gray to brown.

Quantitative optical data have been obtained by microscope spectrophotometry on random sections of polished lindqvistite grains in air and oil (N_d = 1.515). By the courtesy of A. J. Criddle of The Natural History Museum, London, reflectance values were measured in 10-nm steps for the visible spectrum. R values for the four wavelengths recommended by COM are reproduced in Table 1. A second data set, obtained in air at the Swedish Museum of Natural History, gave results in good agreement (Table 1), the systematic differences for the $R_{e'}$ direction merely indicating different orientations of the two grains measured. Color values, calculated from the reflectance data (relative to the CIE illuminant C), confirm the qualitative observations. The relatively small difference in luminance (Y%) for the two measured directions, 22.6–21.8 (air) and 9.10–8.57 (oil), complies with the observed bireflectance. A common dominant wavelength (λ_d) around 480 nm and the low excitation purities (P_e%) at 3.5–2.2 and 7.1–4.7 are in accordance with the lack of perceptible color and dichroism. R values are also given for plumboferrite in Table 1, demonstrating that the difference in overall reflectance is probably the simplest cri-

TABLE 1. Reflectance values (%) in air (R) and oil (^{im}R) for lindqvistite and plumboferrite at the four COM wavelengths

	Lindqvistite						Plumboferrite	
	1				2		3	
λ (nm)	R_o	R_e	$^{im}R_o$	$^{im}R_e$	R_o	R_e	R_o	R_e
470	23.6	22.3	9.97	9.04	23.7	22.0	25.9	24.6
546	22.8	21.9	9.20	8.66	22.7	21.5	24.7	23.8
589	22.2	21.5	8.76	8.34	22.0	21.1	23.9	23.0
650	21.4	21.0	8.20	7.97	21.3	20.7	22.5	22.0

Note: SiC standard from Carl Zeiss Ltd., Oberkochen; 1 = analyst: A.J. Criddle, the Natural History Museum; 2 = analyst: D. Holtstam, Swedish Museum of Natural History; 3 = Criddle and Stanley (1993).

terion for distinguishing these otherwise rather similar minerals.

MINERAL CHEMISTRY

Chemical analyses of the new mineral have been performed by means of energy-dispersive (EDS) as well as wavelength-dispersive (WDS) X-ray spectrometry. An EDS spectrum obtained in a windowless detection mode revealed O as the only element present, with $5 < Z \leq 11$. For the elements with $Z > 11$, WDS data were obtained on a polished single grain using an ARL-SEMQ electron microprobe operated at an acceleration voltage of 15 kV and a beam current of 20 nA with the following standards: metal glass (Pb$M\alpha$), barite (Ba$L\alpha$), rhodonite (Mn$K\alpha$), hematite (Fe$K\alpha$), rutile (Ti$K\alpha$), sphalerite (Zn$K\alpha$), hornblende-type glass (Mg, Al, Si$K\alpha$), and sylvite (Cl$K\alpha$). The counting time per element was 20 s, and raw data were corrected by the MAGIC IV computer program. The same grain was analyzed a second time (after repolishing) with a Cameca SX50 microprobe (20 kV, 12 nA, counting times of 10–40 s, depending on the peak to background ratio of the actual element), utilizing the standard set: vanadinite (Pb$M\beta$), barite (Ba$L\alpha$), pyrophanite (Mn, Ti$K\alpha$), hematite (Fe$K\alpha$), sphalerite (Zn$K\alpha$), periclase (Mg$K\alpha$), corundum (Al$K\alpha$), and wollastonite (Ca, Si$K\alpha$). Data were processed in the Cameca version of the PAP program. The average results of a number of point analyses are given in Table 2. Besides the elements listed, a search for Cr and Sr was made, but the concentrations were below the detection limit (≤0.05%). The two data sets are in good agreement, when one considers the different operating conditions and selection of standards. Results from another lindqvistite specimen are reported as well. The compositions of a number of coexisting oxide minerals were also determined, and selected analyses are given in Table 3.

TABLE 2. Compositional data for lindqvistite

	1a	1b		2
		Oxide wt%		
PbO	25.95	25.76	(25.45–26.32)	25.36
BaO	0.03	0.01	(0.00–0.01)	0.00
CaO	—*	0.00	(0.00–0.00)	0.00
ZnO	0.17	0.00	(0.00–0.00)	0.13
Fe_2O_3	67.49	67.68	(67.26–68.24)	67.71
MnO	5.13	5.13	(5.04–5.20)	6.36
TiO_2	0.12	0.09	(0.05–0.13)	0.05
SiO_2	0.16	0.13	(0.09–0.17)	0.20
Al_2O_3	0.07	0.00	(0.00–0.02)	0.06
MgO	1.62	1.38	(1.30–1.45)	0.56
Cl	0.00	—*		—*
Total	100.74	100.18		100.43
	$n = 6$	$n = 6$		$n = 5$
		19 cations		
Pb	2.04	2.04		2.01
Zn	0.04	0.00		0.03
Fe	14.84	15.01		15.03
Mn	1.27	1.28		1.59
Ti	0.03	0.02		0.01
Si	0.05	0.04		0.06
Al	0.02	0.00		0.02
Mg	0.71	0.61		0.25

Note: 1a = lindqvistite grain (specimen no. 38126) analyzed with the ARL-SEMQ microprobe at the Geological Survey of Sweden (SGU); 1b = the same grain analyzed with the Cameca SX50 probe at Uppsala University (UU) with the analytical ranges given; 2 = lindqvistite grain from sample no. 910048 analyzed at UU; n = number of analyses.
* = Not determined.

TABLE 3. Representative analyses of oxide minerals associated with lindqvistite

	Jacobsite 38126	Hematite 38126	Plumboferrite 38126	Jacobsite 910048
PbO	0.00	0.00	34.00	0.00
ZnO	0.19	0.00	0.00	0.68
FeO*	5.83	—	—	7.81
Fe_2O_3	71.94	99.80	63.54	70.30
MnO	14.24	0.07	2.06	18.70
TiO_2	0.01	0 03	0.11	0.00
SiO_2	0.10	0.00	0.12	0.00
Al_2O_3	0.10	0.00	0.08	0.07
MgO	6.73	0.12	0.17	2.34
Total	99.14	100.02	100.08	99.90

Note: analyses are given in oxide weight percent.
* For jacobsite the number of cations is normalized to 3, then Fe^{2+}/Fe^{3+} is partitioned to balance eight negative charges.

The compositions of a number of coexisting oxide minerals were also determined, and selected analyses are given in Table 3.

To determine the Pb isotopic composition of lindqvistite, 4 mg of the mineral were dissolved in 6 N HCl, and the Pb fraction was purified by ion exchange. The isotope ratios, measured with a Finnigan MAT 261 mass spectrometer and corrected against the NBS standard SRM 981, are $^{206}Pb/^{204}Pb = 15.73 \pm 0.02$, $^{207}Pb/^{204}Pb = 15.38 \pm 0.02$, and $^{208}Pb/^{204}Pb = 35.40 \pm 0.04$.

X-RAY POWDER DIFFRACTION DATA

Powder diffraction patterns of the new mineral were obtained using an automated powder diffractometer. Data were obtained at room temperature in the 2θ range 3–70°; the step width and counting time were 0.01° and 2.5 s, respectively; corrections for systematic errors in the 2θ values were performed against an external Si standard (SRM 640). Intensities, measured as relative peak heights above background, and observed as well as calculated d values, indexed in accordance with space group symmetry $P6_3/mmc$ (see below), are reported in Table 4. The

TABLE 4. X-ray powder diffraction data for lindqvistite

I/I_0	d_{meas} (Å)	d_{calc} (Å)	*hkl*
25	16.64	16.68	002
20	8.33	8.34	004
10	5.55	5.56	006
4	5.095	5.093	101
55	4.168	4.170	008
40	3.334	3.336	0,0,10
60	3.011	3.009	109
70	2.9750	2.9755	110
95	2.8017	2.8004	1,0,10
45	2.7788	2.7798	0,0,12
100	2.6236	2.6234	116
90	2.6125	2.6136	1,0,11
15	2.5101	2.5104	203
15	2.4635	2.4620	204
4	2.3828	2.3827	0,0,14
5	2.3374	2.3380	206
4	2.2675	2.2667	207
10	2.1911	2.1921	208
7	2.1165	2.1158	209
6	2.0845	2.0849	0,0,16
3	2.0399	2.0393	2,0,10
7	2.0313	2.0313	1,1,12
5	1.9636	1.9637	2,0,11
4	1.8527	1.8532	0,0,18
8	1.8386	1.8384	216
10	1.8333	1.8338	1,0,17
20	1.6835	1.6836	2,0,15
15	1.6678	1.6679	0,0,20
15	1.6387	1.6390	2,1,11
15	1.6214	1.6208	2,0,16
3	1.5163	1.5163	0,0,22
10	1.5044	1.5046	2,0,18
25	1.4877	1.4878	220
5	1.4514	1.4509	2,0,19
2	1.3519	1.3522	2,0,21

Note: Philips PW1710 diffractometer, Cu$K\alpha$ radiation.

TABLE 5. Experimental conditions for the crystal-structure analysis of lindqvistite

Space group	$P6_3/mmc$
Unit-cell dimensions (single crystal)	a = 5.952(2), c = 33.379(6) Å
Unit-cell volume, V	1024(1) Å^3
Formula units per unit cell, Z	2
Radiation	Mo$K\alpha$
Wavelength, λ	0.71073 Å
T	293(1) K
Crystal shape	irregular
Crystal size (approx.)	0.34 × 0.20 × 0.06 mm^3
Diffractometer	Stoe four circle
Determination of unit cell:	
No. of reflections used	24
θ range	11.9–12.7°
Intensity data collection:	ω-2θ scan technique
Maximum $\sin(\theta)/\lambda$	0.81/Å
Range of h, k, and l	0–9, −9–9, and 0–53
Standard reflections	3
Intensity instability	3.8%
Internal R	0.048
No. of collected reflections	5339
No. of unique reflections	956
No. of observed reflections	505 (53%)
Criterion for significance	$I > 5\sigma(I)$
Absorption correction:	numerical integration
Linear absorption coefficient	186 cm^{-1}
Transmission factor range	0.09–0.46
Structure refinement:	full-matrix least squares
Minimization of	$\Sigma w \cdot \Delta F^2$
Anisotropic thermal parameters	metal atoms
Isotropic thermal parameters	O atoms
No. of refined parameters	57
Weighting scheme	$[\sigma^2(F) + 0.0005\|F\|^2]^{-1}$
Final R for observed refls.	0.041
Final R_w for observed refls.	0.052
Final R_w for all refls.	0.079
Final $(\Delta/\sigma)_{max}$	0.004
Final $\Delta\rho_{min}$ and $\Delta\rho_{max}$	−2.9 and +2.7 e$^-$/Å^3

figure of merit (Smith and Snyder, 1979) for the present data set is F_{30} = 36.5(0.011,74).

The unit-cell parameters, refined from 25 reflections with 30° < 2θ < 63° by least squares, are a = 5.951(1), c= 33.358(4) Å, and V = 1023.1(5) Å^3 for Z = 2.

Single-crystal X-ray studies

Preliminary work indicated that the new mineral is a hexagonal ferrite with space group $P6_3/mmc$, $P6_3mc$, or $P\bar{6}2c$, and with unit-cell parameters as given above. Accordingly, the structural results and the atomic labeling published for a W-type synthetic ferrite, $BaZn_2Fe_{16}O_{27}$, space group $P6_3/mmc$, a = 5.913 and c = 32.96 Å, (Deschizeaux-Cheruy et al., 1985) were used as an initial structural model of lindqvistite.

Crystal structure analysis

X-ray diffraction data acquired for a selected crystal fragment from sample no. 38126 with a single-crystal diffractometer were corrected for background, Lorentz, polarization, and absorption effects. Further experimental details are summarized in Table 5. The similarity in X-ray scattering powers of Mn and Fe implies that no determination of the proportions of these elements can be obtained from the present data. Subsequently, the symbol Fe will denote the sum of the true Fe and Mn contents. If electroneutrality is assumed, the simplified microprobe-based formula can be written $Pb_2Fe^{2+}_{0.3}Mg^{2+}_{0.7}Fe^{3+}_{16}O_{27}$ in order to be compared with the outcome of the refinements. The final composition, $Pb_{1.82(2)}Mg_{1.0(1)}Fe_{16.2(1)}O_{27}$, obtained from the X-ray study has a slightly lower Pb content (cf. the following) but is otherwise in good agreement. In the initial stages of the least-squares refinement of the structure parameters, each of the metal positions was fully occupied by two types of metal atoms, either Pb and Mg or Fe and Mg. The composition at the metal sites was refined, but in the final structure model mixed sites were only accepted if they were judged to be statistically significant (partial occupancies >3 esd).

A further complication when deriving the structure model is the extensive positional disorder of atoms located at $z \approx$ ¼ (and ¾), which affects the positions of the Pb1, Pb2, Fe5, and O7 atoms. As discussed below, bond distances involving these atoms are considered to have limited physical relevance. The model based on substitution and position disorder could give observable diffraction effects. By exposing X-ray precession photographs for a prolonged time (several days), some rather discrete extra reflections with intensities about two orders of magnitude weaker than the substructure reflections were observed. Although the extra reflections are broader than the main ones, they could be indexed on a hexagonal unit

TABLE 7. Fractional atom coordinates and isotropic displacement parameters for lindqvistite

Atom	Occup.	x	y	z	U_{iso}
Pb1		−0.0473 (2)	−0.0946 (4)	¼	0.0367 (7)
Pb2	82 (2)	0.6269 (2)	0.2538 (2)	¼	0.0142 (5)
Fe1		0	0	0.0555 (1)	0.0053 (5)
Fe2	90 (3)	⅓	⅔	−0.4264 (1)	0.0050 (6)
Fe3		⅓	⅔	0.0920 (1)	0.0045 (4)
Fe4	95 (2)	−0.1644 (1)	−0.3288 (2)	0.1485 (1)	0.0067 (4)
Fe5		⅓	⅔	0.2043 (1)	0.0174 (7)
Fe6	90 (2)	½	0	0	0.0071 (5)
O1		−0.1758 (6)	−0.3516 (12)	0.0359 (2)	0.0086 (11)
O2		⅓	⅔	0.0337 (4)	0.0060 (19)
O3		0.5117 (6)	0.0234 (1)	0.1097 (2)	0.0078 (11)
O4		0	0	0.1138 (4)	0.0085 (20)
O5		0.1649 (6)	0.3298 (12)	0.1783 (2)	0.0063 (11)
O6		⅓	⅔	−0.3227 (4)	0.0108 (23)
O7		0.4790 (20)	0.9580 (40)	¼	0.0827 (90)

Note: for the metal atoms for which an occupancy (%) is given, the remaining content to give 100% metal occupancy was refined as Mg. The equivalent isotropic displacement parameters for the atoms for which anisotropic displacement factors were refined (all metal atoms and the atom O7) were estimated as ⅓·trace(**U**).

cell that is three times larger. The new unit-cell vectors are obtained by the transformation matrix ($\mathbf{T}_a$)

$$\mathbf{T}_a = \begin{Bmatrix} 2 & 1 & 0 \\ -1 & 1 & 0 \\ 0 & 0 & 1 \end{Bmatrix}.$$

The new unit-cell parameters obtained by the transformation are $a' = a \cdot \sqrt{3} = 10.31$ Å, whereas $c' = c = 33.36$ Å. Transforming the present structure model into the superstructure shows that most of the atom positions of the $P6_3/mmc$ substructure are less restricted by symmetry or split into two independent positions or both. Attempts to obtain an X-ray intensity data set that includes the more intense extra reflections have recently been initiated but are hampered partly by the large reflection widths. It should also be pointed out that the cell-subcell relationship described is identical with the results of Kohn and Eckart (1969), whose work was not available to us during the experiments.

The final least-squares refinement of the substructure, using anisotropic displacement parameters for all metal ions and for the disordered O atom O7 but isotropic ones for the remaining O atoms, gave an R value of 0.041 (weighted $R_w = 0.079$ for all reflections). Observed and calculated structure factor amplitudes are reproduced in Table 6A.[1] The final atom coordinates are given in Table 7, together with isotropic displacement parameters. The anisotropic displacement parameters are summarized in Table 6B,[1] and the most relevant interatomic distances in Table 8. The structure refinements were performed with the SHELX-76 program package (Sheldrick, 1976), using atomic scattering factors for neutral atoms from *International Tables for X-ray Crystallography* (Ibers and Hamilton, 1974).

[1] A copy of Tables 6A and 6B may be ordered as Document AM-93-541 from the Business Office, Mineralogical Society of America, 1130 Seventeenth Street NW, Suite 330, Washington, DC 20036, U.S.A. Please remit $5.00 in advance for the microfiche.

Description of the structure

The substructure of lindqvistite (Fig.2) is isotypic with the W-type hexagonal ferrite structure, which consists of stacks along the **c** axis of two types of blocks, designated *S* (spinel) and *R*. The two types of blocks are obtained when approximately cubic and hexagonal closest-packed layers of the larger O and *A* atoms are stacked (with smaller cations occupying the voids formed). The block sequence of the W-type ferrite (and lindqvistite) can be denoted *RSSR'S'S'*. The primed blocks are rotated 180° relative to the unprimed ones because of the space group symmetry operations. With the notations *hhh* and *cc* for the hexagonal and cubic closest-packed layer sequences, respectively, of the *R* block (three layers) and the *S* block (two layers), the close-packing can be written symbolically (·*cchhhcccchhhcc*·). Note that, in lindqvistite, only one of the symmetry-independent Pb atoms, replacing one of four O atoms in every seventh layer, is involved in the closest-packing.

Both Pb positions, Pb1 and Pb2, and one of the O positions, O7, which are located in the central section (z = ¼) through the *R* block (Fig. 3a, 3b), are disordered. With the adopted structure model, the electron density distribution (Fig. 3c) is approximately ellipsoid shaped. However, the observed electron density distributions at the two symmetry-independent Pb atomic positions are far from ellipsoidal, and accordingly the Pb positions were split. From Figure 3c it appeared reasonable to split each Pb position into a triplet (cf. Fig. 3b). No indications were found for deviations of the Pb atom positions from the mirror plane at $z = \pm$¼. Thus, the Pb1 atom was allowed to deviate from the symmetry-restricted (0,0,¼) position ($\bar{6}m2$ point symmetry) by locating it in a less restricted (x, $2x$, ¼) position ($mm2$ symmetry) with a positional occupancy of ⅓. Similarly, the Pb2 atom was also located in a (x, $2x$, ¼) position with ⅓ occupancy instead of in the more restricted (⅔, ⅓, ¼) position ($\bar{6}m2$ symmetry). The calculated interatomic distances, listed in Table 8, simply reflect the distances between the ellipsoid cen-

TABLE 8. The shortest metal-O distances (Å) with estimated standard deviations and multiplicities for the coordination polyhedra of lindqvistite

Coordination	Atoms	Distance	Multiplicity
R_{8+4}	Pb1-O7	2.595 (16)	× 2
	-O5	2.834 (6)	× 4
	-O7′	2.989 (16)	× 2
	-O5′	3.243 (6)	× 2
	-O7″	3.430 (16)	× 2
R_5	Pb2-O7	1.525 (16)	× 1
	-O7′	2.169 (23)	× 2
	-O6	2.462 (8)	× 2
S_4	Fe1-O1	1.927 (7)	× 3
	-O4	1.946 (8)	× 1
S_6	Fe2-O3	2.002 (7)	× 3
	-O1	2.056 (7)	× 3
S_4	Fe3-O3	1.937 (7)	× 3
	-O2	1.946 (7)	× 1
$(RS)_6$	Fe4-O5	1.968 (6)	× 2
	-O6	1.990 (8)	× 1
	-O4	2.053 (8)	× 1
	-O3	2.117 (7)	× 2
R_6	Fe5-O5	1.942 (7)	× 3
	-O7	2.141 (16)	× 3
$(SS)_6$	Fe6-O2	2.054 (8)	× 2
	-O1	2.058 (7)	× 4

Note: *R* and *S* denote coordination polyhedra within the two types of structural blocks of the lindqvistite structure. *RS* denotes a polyhedron common to adjacent *R* and *S* blocks and *SS* a polyhedron common to two *S*. The subscripts denote the coordination numbers of the metal positions.

troids. Because of static and dynamic disorder, these centroids represent, when determined from single-crystal diffraction data, positional distributions averaged over crystal space and time. Accordingly, any distances calculated by using the centroid positions of such distributions should not be expected to give realistic bond distance estimates. A particularly unrealistic value of 1.53 Å is obtained for the Pb2-O7 distance, indicating that the coordination around Pb2 is rather undefined. The split Pb1 positions are located at the corners of small equilateral triangles (Fig. 3b), with sides of 0.84 Å, at a distance of 0.49 Å from the ideal position. For Pb2 the corresponding distances are 0.71 and 0.41 Å, respectively. The metal to metal contact of 2.77 Å, which is the shortest distance obtained between split Pb1 and Pb2 positions, should be considered to have but little physical relevance. The shortest O-O distance in the structure is the one between symmetry-related O7 positions, which is as small as 2.60 Å. Apart from any effects of positional disorder of O7, this distance can be expected to be shortened also as the O7 atoms form a shared face between two Fe5 octahedra.

Note that the coordination number around the ideal Pb1 position (0,0,¼) is 12 (twinned cuboctahedron) with distances ranging only from 2.94 to 2.98 Å, whereas the eightfold coordination around the observed Pb1 position gives distances (possibly affected by disorder) from 2.60 to 2.99 Å (Table 8). If the four more distant O atoms (2 × 3.24 and 2 × 3.43 Å) around Pb1 are considered, the

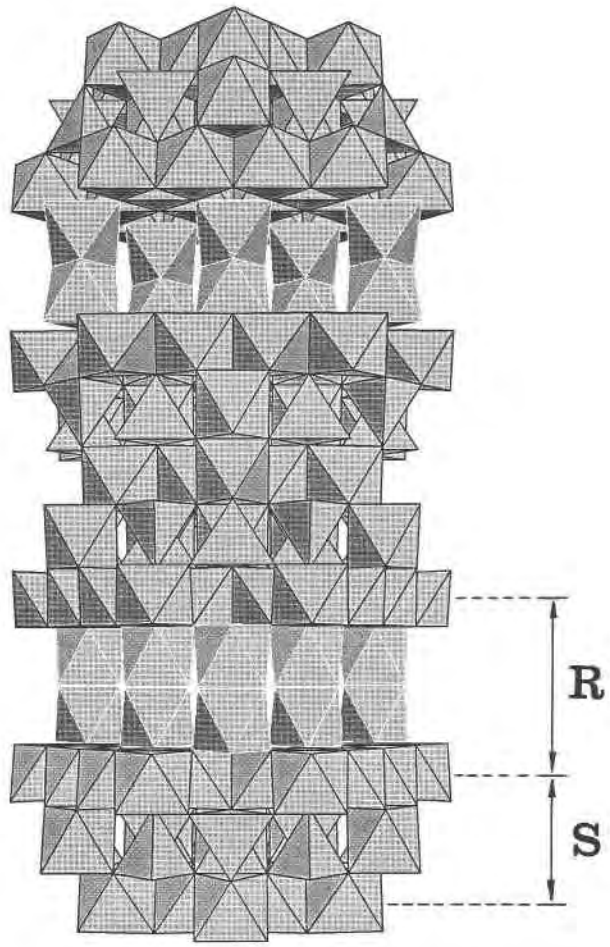

Fig. 2. The lindqvistite structure viewed approximately along the perpendicular to [001]. The polyhedra packed as in the spinel structure are drawn with black edges, and the face-sharing octahedra around $z = ¼$ are drawn with white edges. The structural entities defining the *R* and *S* blocks are indicated. For clarity, the Pb atoms and their coordination polyhedra, located in the central section through the *R* block, are omitted.

12-fold-coordination distance range extends up to 3.43 Å. The empirical bond-valence sums calculated with the parameters for Pb compiled by Brown and Altermatt (1985) at the ideal and the observed Pb1 positions are 1.22 and 1.45, respectively, suggesting that the observed Pb1 position receives a bond-valence sum closer to +2. Including the minor Mg content of the Pb2 position would only lower the bond-valence sum marginally.

The Mg content at the Pb2 position probably has limited relevance. Assume that the observed disordered electron density around the Pb2 position (Fig. 3c) is not completely describable as a sum of ellipsoid-shaped contributions of pure Pb with centroids at the split Pb2 positions. In such a case the sum of occupancies would be <100%, even if there were no real vacancies, and a difference electron-density calculation would give a significant residue in the vicinity of the Pb2 position. A total occupancy of 100% could, of course, still be obtained in

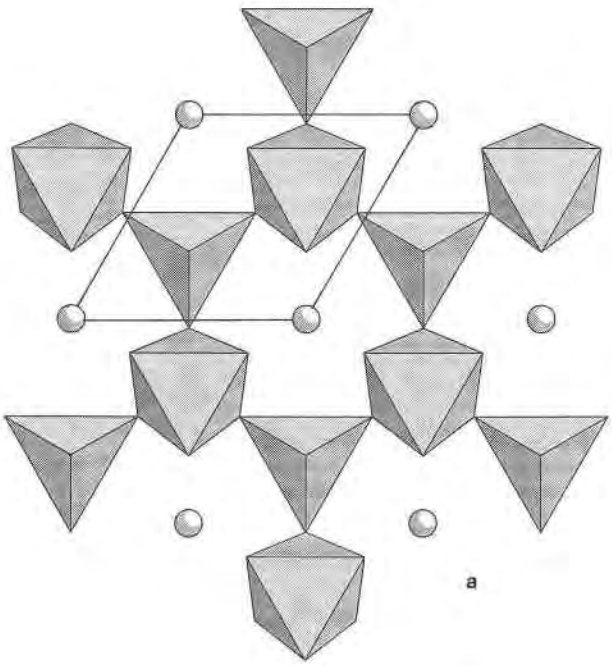

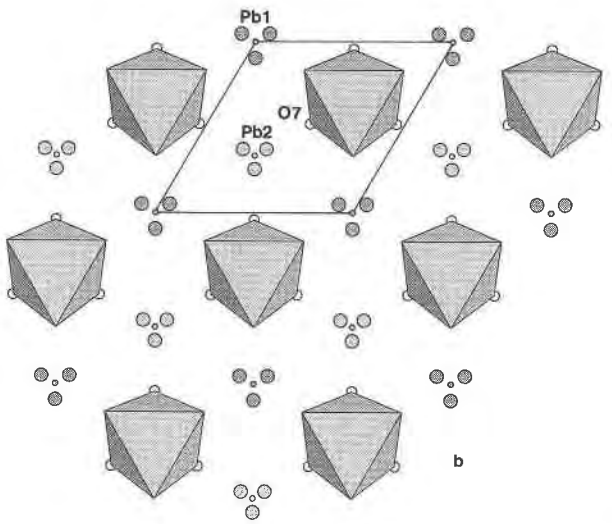

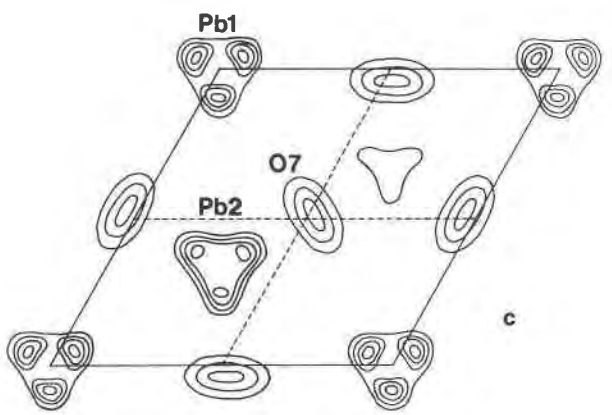

the least-squares refinement by assuming a mixture of Pb and Mg instead. Such a model was used in the present study, simply to avoid introducing vacancies into the model that might lead to unnecessary and more serious confusion about the derived structure model. Some indication that the Pb2 position might consist of pure Pb is offered by a peak in the calculated $\Delta\rho$ map close to the split Pb2 positions, with a height ($+2.1$ e$^-$/Å^3) above the background level (estimated to 1.2 e$^-$/Å^3). If this indication is valid, the refined chemical formula changes from $Pb_{1.8}Mg_{1.0}Fe_{16.2}O_{27}$ to $Pb_{2.0}Mg_{0.8}Fe_{16.2}O_{27}$, in remarkably good agreement with the microprobe-based values of Table 2. Apart from the slightly dubious Mg content at the Pb2 positions, significant amounts of Mg were only indicated at the octahedrally coordinated Fe positions Fe2, Fe4, and Fe6 (Tables 6B and 7).

To assess the relevance of the structure model obtained in this study, bond-valence sum values were also calculated for the Fe positions, assuming occupancy only of Fe. Taking the minor Mg content into account would only lower the estimated bond-valence sum values marginally. These values range from 2.69 to 2.90 for the [6]Fe positions (2, 4, 5, and 6). Slightly lower bond-valence sum values of 2.46 and 2.51 are obtained for the tetrahedrally coordinated metal positions (1 and 3, respectively). As similar values are also obtained for the structure determined, e.g., by Deschizeaux-Cheruy et al. (1985), for the closely related ferrite $BaZn_2Fe_{16}O_{27}$ (2.70–3.09 for octahedral, 2.40 and 2.58 for tetrahedral coordinations), the Fe and most of the O positions obtained in the present study seem to be valid, despite the observed disorder in the central section of the *R* block.

Discussion

Although the substructure of lindqvistite is isotypic with the W-type structure of synthetic ferrites, as suggested by Kohn and Eckart (1969) and confirmed by this study, no phase equivalent to lindqvistite has been found in the intensively studied system BaO-*Me*O-Fe_2O_3 (Fig. 4). This is probably a result of the difference in ionic radii between Ba^{2+} (1.43 Å) and Pb^{2+} (1.32 Å), and their different crys-

←

Fig. 3. (**a**) A projection along [001] of an idealized *R* block in lindqvistite. The face-sharing octahedra around Fe5 and the trigonal bipyramid around the ideal position of Pb2 are drawn. The ideal Pb1 positions (12-fold coordinated) are shown as circles. The indicated unit cell has its origin in the upper left corner. (**b**) Similar projection as in **a**, but showing both the disordered Pb positions (larger circles) and the ideal Pb positions (smaller circles) at $z = \frac{1}{4}$. The position of O7, which also participates in the coordination of the Fe5 atoms, is indicated. (**c**) The observed $\Delta\rho$ map for $z = \frac{1}{4}$ with an orientation similar to that in **a** and **b**, calculated by omitting any contributions from the Pb1, Pb2, and O7 atoms. The contour intervals are 10 e$^-$/Å^3 for Pb and 2 e$^-$/Å^3 for O, respectively. The map clearly indicates the disorder of the omitted atoms.

tal chemical behavior due to dissimilar electron configurations. Ba^{2+} has the Xe noble gas configuration, whereas Pb^{2+} has a lone pair of stereoactive $6s^2$ electrons. It seems likely that a major factor behind the observed disorder in the lindqvistite structure is related to the anomalous lone-pair effect. Splitting of Pb among symmetry-equivalent sites has been analyzed and described in detail by Moore et al. (1989) for synthetic magnetoplumbite and other Pb-bearing oxysalts. In magnetoplumbite each Pb atom is equally distributed over six positions (m symmetry), displaced 0.31 Å from a fixed point; compare $BaFe_{12}O_{19}$, where refinement showed that Ba is at a symmetry-fixed site with $\bar{6}m2$ symmetry (Obradors et al., 1985). Unfortunately, there seems to be no other investigation of phases in the system PbO-MeO-Fe_2O_3. There is also an interesting parallel in the relationship between the structures of magnetoplumbite (M) and plumboferrite as for synthetic W and lindqvistite. In the same way as lindqvistite is a derivative of the W structure type, the subcell of plumboferrite is geometrically identical to that of M (Kohn et al., 1968). In both cases, however, the result is an increase in the A-type atom content of the phase when going from the structures of true M and W to the derivatives.

The packing efficiency in terms of closest-packed atoms (V_E) in the unit cell is 18.8 Å^3/(O^{2-} + $^{[8+4]}Pb^{2+}$) for lindqvistite, a somewhat less dense value than for W-type $BaZn_2Fe_{16}O_{27}$ [V_E = 17.8 Å^3/(O + Ba)] and magnetoplumbite [V_E = 17.2 Å^3/(O + Pb)]. The introduction of an extra A-type atom in the structure that is not subject to closest-packing clearly influences V_E for lindqvistite. However, in the heated and quenched sample a reduction in the cell parameters to ca. a = 5.92 and c = 32.96 Å was observed. It has evidently undergone some structural changes, manifested by a change in magnetic properties and cell volume (by −2.3%, which gives V_E = 17.8 Å^3).

The oxidation states assumed here for the elements, Mn^{2+} and Fe^{3+}, are inferred from the compositions of coexisting oxide phases (Table 3). The hematite is essentially pure Fe_2O_3, and the jacobsite contains 18–25% Fe_3O_4, indicating an f_{O_2} level at which only Mn^{2+} is stable. A preliminary Mössbauer spectroscopy investigation of lindqvistite showed no trace of Fe^{2+}. When one calculates a structure formula for lindqvistite based on the microprobe analyses, it appears that the proportion of quadrivalent species cannot balance the surplus of Me^{2+} ions (for 2 × 27 O atoms in the unit cell), unless there is some Pb^{4+}. However, it is well documented from HRTEM studies on synthetic hexagonal ferrites (van Landuyt et al., 1974) that defects at the atomic level, such as stacking faults, are frequent and seriously affect the stoichiometry of these compounds.

The element partitioning between phases also deserves some comment. Lindqvistite is enriched in Mn over Mg relative to coexisting jacobsite, and Mn is even more favored by plumboferrite. A distribution coefficient of ~1.5 for the Mn/Mg ratio occurs in both lindqvistite-jacobsite pairs, suggesting chemical equilibrium for the assemblage. The general appearance and the mineralogical composition of the lindqvistite-bearing samples suggest that they have formed at peak metamorphic conditions, estimated at a minimum of 680 °C (inferred from the presence of periclase at the deposit, evidently formed by dissociation of carbonate). The Pb isotope composition of lindqvistite falls well within the ranges of isotopic signatures for Långban-type deposits given by Åberg and Charalampides (1986). The calculated two-stage evolution model age (Faure, 1986) of 1.82 Ga is in reasonable agreement with the assumed geological age.

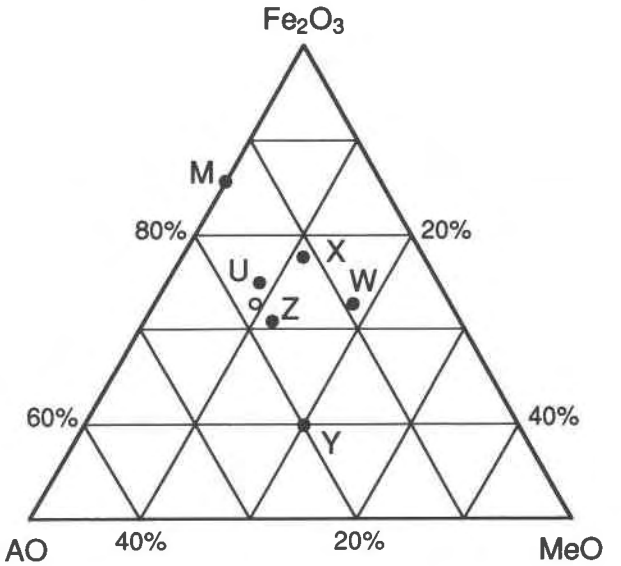

Fig. 4. Part of the ternary system AO-MeO-Fe_2O_3 for A = Ba (molar percentages). The letter designations of different phases originate from Braun (1957). The composition of lindqvistite (A = Pb) is shown by an open circle.

As regards the intracrystalline ion distribution, the pattern for Mg^{2+} obtained by the structure refinements is somewhat different compared with synthetic W-type $BaMg_2Fe_{16}O_{27}$, where Mg is distributed over the octahedral and tetrahedral sites in the spinel layer, i.e., site nos. 1, 2, 3, and 6 (Collomb et al., 1986). For lindqvistite it appears to be a fair assumption that Mn^{2+} is concentrated at the tetrahedral sites, if one considers the fact that the simple spinel $MnFe_2O_4$ (jacobsite) is largely normal and bears in mind the lower bond-valence sums obtained for these sites. The Mössbauer spectrum (at 300 K), displaying magnetic splitting, is resolved into two sextets, provisionally attributed to the Fe1 + Fe2 + Fe3 + Fe5 + Fe6 and Fe4 sites, respectively. The Mössbauer characteristics and magnetic properties of lindqvistite and related minerals will be addressed in future work.

Finally, the formation of Pb-bearing ferrites in nature requires, apart from appropriate bulk compositions, low activities of S and Si, and relatively high f_{O_2} values. As these conditions are seldom fulfilled in the geological environment, the minerals are expected to be exceedingly rare. However, considering the prolific nature of the fer-

rite family, there is a possibility that more phases in this system can be found if systematic investigations are carried out on material from Jakobsberg and deposits of similar geochemical character.

Acknowledgments

The authors are indebted to A. Sjödin, Stockholm University, for his assistance with the X-ray photographic investigations, and to A.J. Criddle, The Natural History Museum, London, for providing reflectance data. Critical reviews by J.A. Kohn and P.B. Moore are highly appreciated. This work has been supported financially by the Swedish Natural Science Research Council (NFR).

References cited

Åberg, G., and Charalampides, G. (1986) New lead isotope data from the Långban mineralization, central Sweden. Geologiska Föreningens i Stockholm Förhandlingar, 108, 243–250.

Björk, L. (1986) Beskrivning till Berggrundskartan Filipstad NV. Sveriges Geologiska Undersökning, Af 147, 1–110.

Boström, K., Rydell, H., and Joensuu, O. (1979) Långban: An exhalative sedimentary deposit? Economic Geology, 74, 1002–1011.

Braun, P.B. (1952) Crystal structure of $BaFe_{18}O_{27}$. Nature (London), 170, 708.

——— (1957) Crystal structures of a new group of ferromagnetic compounds. Philips Research Reports, 12, 491–548.

Brown, I.D., and Altermatt, D. (1985) Bond-valence parameters obtained from a systematic analysis of the inorganic crystal structure database. Acta Crystallographica, B41, 244–247.

Collomb, A., Abdelkader, O., Wolfers, P., and Guitel, J.C. (1986) Crystal structure and magnesium location in the W-type hexagonal ferrite [Ba]Mg_2-W. Journal of Magnetism and Magnetic Materials, 58, 247–253.

Collongues, R., Gourier, D., Kahn-Harari, A., Lejus, A.M., Théry, J., and Vivien, D. (1990) Magnetoplumbite-related oxides. Annual Review of Materials Science, 20, 51–82.

Criddle, A.J., and Stanley, C.J. (1993) Quantitative data file for ore minerals (3rd edition), 698 p. Chapman and Hall, London.

Damman, A.H. (1988) Exhalative-sedimentary manganiferous iron ores from the Gåsborn area, W. Bergslagen, Central Sweden. Geologie en Mijnbouw, 67, 433–442.

Deschizeaux-Cheruy, M.N., Vallet-Rigi, M., and Joubert, J.C. (1985) Structure d'un ferrite hexagonal: La phase $(Zn_2)W$, $BaZn_2Fe_{16}O_{27}$ stoechiometrie du composé. Journal of Solid State Chemistry, 57, 234–239.

Faure, G. (1986) Principles of isotope geology, 589 p. Wiley, New York.

Ibers, J.A., and Hamilton, W.C. (1974) International tables for X-ray crystallography, vol. IV., 366 p. Kynoch, Birmingham, U.K.

Kohn, J.A., and Eckart, D.W. (1969) Evidence for a mineral series in the plumboferrite group. Geological Society of America Abstracts with Programs, 1, 127–128.

Kohn, J.A., Peacor, D.R., and Eckart, D.W. (1968) Plumboferrite: Cell, symmetry, and basic structure. Geological Society of America Abstracts with Programs, 162–163.

Kojima, H. (1982) Fundamental properties of hexagonal ferrites. In E.P. Wohlfahrt, Ed., Ferromagnetic materials, vol. 3, p. 305–391. North-Holland, Amsterdam.

Moore, P.B. (1970) Mineralogy and chemistry of Långban-type deposits in Bergslagen, Sweden. Mineralogical Record, 1, 154–172.

Moore, P.B., Sen Gupta, P.K., and Le Page, Y. (1989) Magnetoplumbite, $Pb^{2+}Fe^{3+}_{12}O_{19}$: Refinement and lone-pair splitting. American Mineralogist, 74, 1186–1194.

Obradors, X., Collomb, A., Pernet, M., Samaras, D., and Joubert, J.C. (1985) X-ray analysis of the structural and dynamic properties of $BaFe_{12}O_{19}$ hexagonal ferrite at room temperature. Journal of Solid State Chemistry, 56, 171–181.

Sheldrick, G.M. (1976) SHELX-76: Program for crystal structure determination. University of Göttingen, Göttingen, Germany.

Smith, G.S., and Snyder, R.L. (1979) F_N: A criterion for rating powder diffraction patterns and evaluating the reliability of powder-pattern indexing. Journal of Applied Crystallography, 12, 60–65.

Tegengren, F.R. (1924) Sveriges ädlare malmer och bergverk. Sveriges Geologiska Undersökning, Ca 17, 1–406.

van Landuyt, J., Amelinckx, S., Kohn, J.A., and Eckart, D.W. (1974) Multiple beam direct lattice imaging of the hexagonal ferrites. Journal of Solid State Chemistry, 9, 103–119.

Manuscript received January 5, 1993
Manuscript accepted July 5, 1993